Crystallization Behavior of a Thermoplastic Polyimide Derived from 3,3′,4,4′-Oxydiphthalic Dianhydride and 4,4′-Oxydianiline

Guiyan Zhao,[1,2] Min Zhang,[1,2] Yongfeng Men,[1] Mengxian Ding,[1] Wei Jiang[1]

[1]State Key Laboratory of Polymer Physics and Chemistry, Changchun Institute of Applied Chemistry, Chinese Academy of Sciences, Changchun 130022, People's Republic of China
[2]Graduate School of the Chinese Academy of Sciences, Beijing 100039, People's Republic of China

ABSTRACT: Nonisothermal and isothermal crystallization kinetics of an aromatic thermoplastic polyimide derived from 3,3′,4,4′-oxydiphthalic dianhydride and 4,4′-oxydianiline have been investigated by means of differential scanning calorimetry (DSC) and wide-angle X-ray diffraction. The results for nonisothermal crystallization study showed that a weak melting peak appeared during the first heating process, whereas no crystallization peak appeared in the DSC curve during the subsequent cooling process. On the other hand, the study for the isothermal crystallization in the temperature range of 260–330°C showed that a new exothermic peak appeared at lower temperature for the samples crystallized for 100 min at 300°C. Moreover, the results indicated that the crystallization behaviors were largely affected by the crystallization temperature and crystallization time. During the annealing process, the melting enthalpy tended to increase with increasing annealing temperature and annealing time. More interesting was that two melting endotherms appeared when the annealing temperature was lower than 300°C. However, when the annealing temperature was higher than 330°C, only one melting endotherm appeared. © 2008 Wiley Periodicals, Inc. J Appl Polym Sci 108: 1893–1900, 2008

Key words: polyimides; crystallization; annealing

INTRODUCTION

Aromatic polyimides possess some distinct properties such as marked thermal stability, high electrical and solvent resistance, etc. Therefore, polyimide materials have special applications in automobile and aircraft parts and packaging imprinted electronic circuitry, and continue to gain importance in a wide variety of applications like high-temperature adhesives and composites, microelectronics, membranes, and as photosensitive materials.[1–3] In general, introduction of crystallinity in these materials can further substantially improve the thermal stability and enhance solvent resistance,[4–6] as well as increase radiation resistance and partial retention of mechanical properties above the T_g.[7,8] Therefore, semicrystalline polyimides have been the focus of considerable research over the recent years.[9–29] Although many polyimides have been reported to exhibit crystallinity, most do not recrystallize, once taken to the melt. Side reactions like crosslinking branching or chain scission, which may occur at these high melt temperatures, usually lead to build up in the molecular weight. This can change the rheology and the crystallization behaviors.[6] Among the few polyimides that do show some evidence of crystallization from the melt, the recrystallization ability decreases rapidly with increasing times and temperatures in the melt, while in most cases, it was not possible to attain any crystallinity in the polyimide once it was taken to melt temperature. Thus, considerable efforts have been devoted to developing semicrystalline polyimides which display sufficient thermal and recrystallization stability. There are many studies reported on the crystallization behavior and kinetic of these semicrystalline polyimides. However, most polyimides cannot recrystallize, and less effort was focused on the crystallization behavior of these aromatic polyimides that maintain reasonably high strength and thermal stability but cannot recrystallize. Aromatic thermoplastic polyimide derived from 3,3′,4,4′-oxydiphthalic dianhydride (3,3′,4,4′-ODPA)
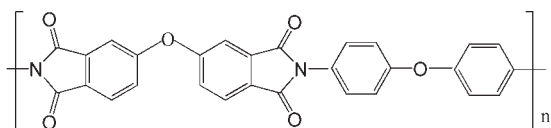
Figure 1 Chemical structure of the polyimide (PI) derived from 3,3′,4,4′-oxydiphthalic dianhydride (3,3′,4,4′-ODPA) and 4,4′-oxydianiline (ODA).

and 4,4′-oxydianiline (ODA) is processed and used as amorphous materials. It is usually coated as varnish or spun-cast as thin films, from the poly(amic acid) precursor, and then thermally imidized *in situ*. The rigidity of the chains results in high glass transition temperatures and often leads to a decomposition temperature that is reached before the crystal melting point. This makes them extremely difficult to melt-process and recrystallize. So, it is important from both a fundamental and practical standpoint to study the crystallization behavior of the polyimide.

In this article, we have studied the nonisothermal and isothermal crystallization kinetics of an aromatic thermoplastic polyimide derived from 3,3′,4,4′-ODPA and ODA. The purpose is to give an insight into the crystallization behavior for the polyimide.

EXPERIMENTAL

Materials

The thermoplastic polyimide powder, which was synthesized from 3,3′,4,4′-oxydiphthalic dianhydride (3,3′,4,4′-ODPA) and 4,4′-oxydianiline (ODA), was prepared by ourselves. The detailed synthetic procedures of the polyimide have been reported elsewhere.[29] Inherent viscosity of the polyimide in *m*-cresol at 0.5 g/100 mL at 303 K was measured. The inherent viscosity of the polyimide varied from 0.34 to 0.55 dL/g with the variation of the endcapper phthalic anhydride (PA). The sample with typical inherent viscosity of 0.46 dL/g was used for basic study. The chemical structure of the PI is shown in Figure 1. All materials were dried under vacuum for 24 h at 120°C prior to use.

Differential scanning calorimetry

Differential scanning calorimetry (DSC) measurements were carried out to characterize the thermal properties of the sample using Perkin–Elmer DSC-7. The amount of polymer utilized in a given thermal scan was kept at 10 ± 0.2 mg. The DSC was calibrated with indium and zinc standards at the heating rate utilized. All experiments were conducted under a nitrogen purge, and a DSC baseline was determined by running empty pans. For nonisother-
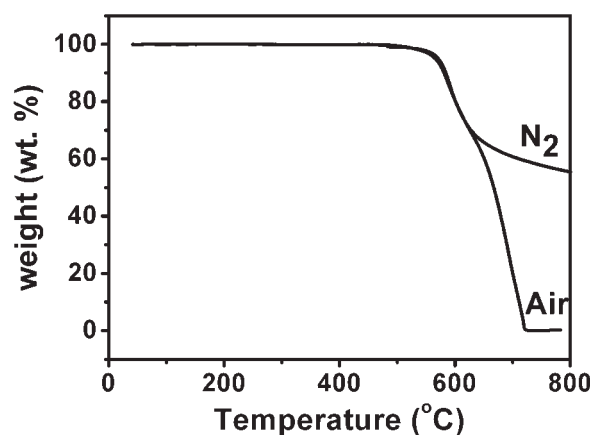
Figure 2 Percentage weight loss as a function of temperature in nitrogen and air for the PI at a heating rate of 20°C/min.

mal crystallization study, samples were heated from 50 to 400°C or cooled from 400 to 50°C at 20°C/min. For isothermal crystallization kinetics study, the samples were first heated to melt temperature and kept for 1 min, then cooled at 50°C/min to predetermined temperatures of 260, 300, and 330°C. As to the transition with a low heat for the crystallization study, the samples were heated to different melt temperature and kept for 1 min, then quickly cooled to crystallization temperature, and the subsequent heating curves at 20°C/min were recorded after the samples were isothermally crystallized at 330°C for different periods of time. To investigate the effect of annealing, several annealing temperatures were selected. After annealing for different periods of time, samples were cooled to room temperature, and then heated to 400°C at 20°C/min. Heating curves were recorded.
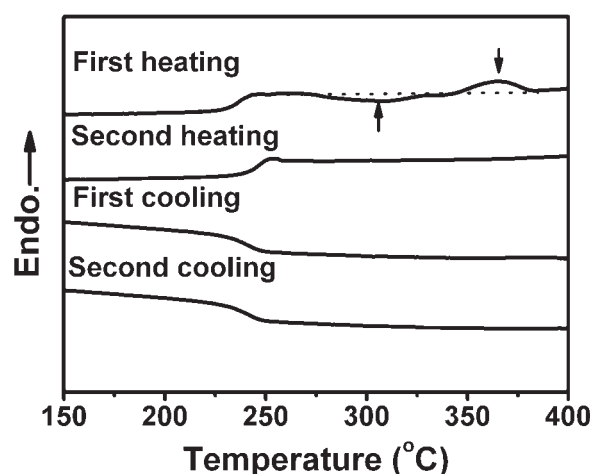
Figure 3 Consecutive DSC heating scans of the PI for the first and second heating and cooling at a rate of 20°C/min.
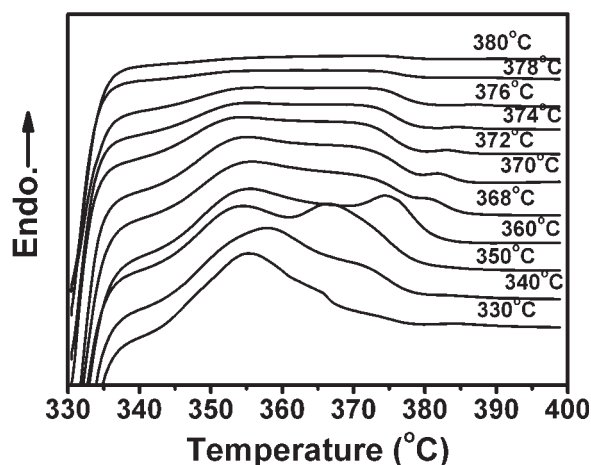
Figure 4 DSC subsequent heating curves of the PI crystallized at 330°C for 50 min with different melting temperatures.

Wide-angle X-ray diffraction

The wide-angle X-ray diffraction (WAXD) for samples was measured by a Rigaku D/Max 2500V PC X-Ray Diffractometer (Cu Kα radiation λ = 1.5406 Å, generator voltage = 40 kV, current = 200 mA). Data were collected during continuous scans, at a speed of 4°/min from 5 to 40°.

Small-angle X-ray scattering

Small-angle X-ray scattering (SAXS) was performed at BW4, HASYLAB at DESY, Hamburg, Germany. The X-ray wavelength was λ = 1.3808 Å. The sample-to-detector distance was L_{SD} = 3938 mm. The effective scattering vector q ($q = 4\pi \sin \theta/\lambda$, where 2θ is the scattering angle) at this distance ranges from 0.1 to 1.0 nm^{-1}. Scattering data was corrected for background scattering and normalized with respect to the primary beam intensity.

Thermogravimetric analysis

Thermogravimetric analysis (TGA) was carried out on a Perkin–Elmer 7 series thermal analysis system (United States). TGA scans were recorded at 20°C/min under an air atmosphere from 50 to 800°C. The temperature was calibrated using indium and zinc standards.

RESULTS AND DISCUSSION

Thermal stability

Figure 2 shows the weight loss of the polyimide, with temperature in air and nitrogen from TGA measurement, respectively. It can be seen that the weight remains roughly unchanged below 500°C. The 5% weight loss temperatures in air and nitrogen are 564°C and 572°C. It indicates that the sample possesses very good thermal stability both in air and nitrogen.

Nonisothermal crystallization

To understand the initial melting behavior and recrystallization response once heated above the T_m, DSC experiments were conducted by heating the samples to a melting temperature of 400°C for 1 min. Two consecutive scans are shown in Figure 3. The initial material is amorphous PI. During the first heating, it displays a predominant glass transition temperature at 246°C. Although the material is initially amorphous and difficult to crystallize, it can crystallize somewhat during first heating process. From Figure 3 we can see a weak crystallization endotherm appeared at 308°C. Therefore, the melting endotherm with endothermic peak at 365°C should results from the crystallization of the sample during the heating process. During the cooling process, no exothermic peak is found. During the subsequent heating process, the weak endothermic peak disap-
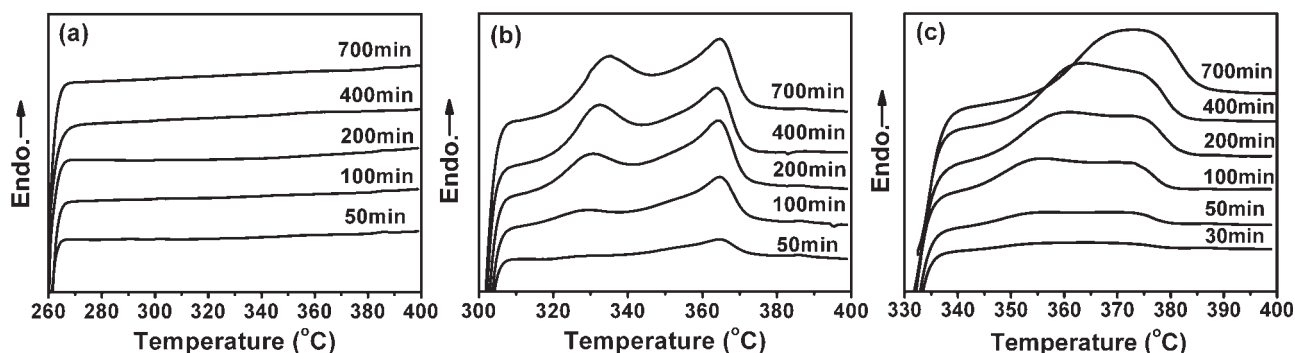
Figure 5 DSC subsequent heating curves of the PI isothermally crystallized at (a) 260°C, (b) 300°C, (c) 330°C for different times.
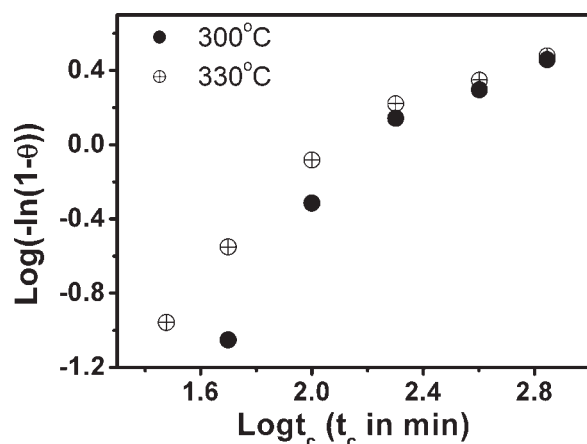
Figure 6 Avrami plot of the PI isothermally crystallized at 300°C and 330°C.

pears accordingly. Although the TGA result showed that the 5% weight loss temperature in air and nitrogen are 572°C and 564°C, respectively, the consecutive DSC scans show that a thermogravimetric experiment is not the best means to evaluate the thermal stability for the polyimide. Crosslinking and chain-branching reactions may occur above the melting temperature of the polymer without any significant weight loss. This can be confirmed from the rheological results, which shows that the complex viscosity for this PI increases gradually with increasing temperature when the temperature is higher than 360°C.[29] To study the effect of melting temperature on the crystallization, the sample was heated to different melting temperature and kept for 1 min, and then cooled to 330°C and crystallized for 50 min. Figure 4 shows the subsequent heating DSC curves for the crystallized samples at 20°C/min. The total enthalpy is continually increased with increasing the melting temperature up to 350°C, thereafter it decreases slowly with further increase in the melt temperature. When the melting temperature is increased to 380°C, no endothermic peak appeared.

The results indicate that the recrystallization of the PI sample used in this study is largely affected by melting temperature. An appropriate melting temperature is very important for the recrystallization of the PI sample.

Isothermal crystallization

To eliminate the thermal history from the sample preparation and maintain the recrystallization ability, 376°C was selected as the melt temperature for the isothermal crystallization study. Avrami analysis is the most widely used means of describing the overall bulk isothermal crystallization of polymers, although it is associated with various experimental[30] and theoretical complications.[31–34] The Avrami equation is generally written as

$$\theta = 1 - \exp(-kt^n) \qquad (1)$$

where θ is the crystallized fraction in material, k and n are Avrami constants and are indicative of the crystallization mechanisms involved. k is a temperature-dependent rate constant, and it is dependent upon the dimensionality of the growing crystalline entities (e.g., whether they are spheres, discs, or rods), t represents time, and n describes the mode of nucleation and crystal growth and usually is an integer between 1 and 4 for different crystallization mechanisms. It has also been observed that n is a fraction due to secondary crystallization or crystal perfection. Isothermal DSC is the primary means of performing such an analysis, and θ is expressed as

$$\theta = \frac{\Delta H_t}{\Delta H_0} = \frac{\int_0^t E_t \, dt}{\int_0^\infty E_t \, dt} \qquad (2)$$

where ΔH_t is the fractional heat of fusion after crystallization time t, ΔH_0 is the total heat of crystallization observed at the isothermal crystallization temperature, and E_t is the rate of energy evolution at time t.
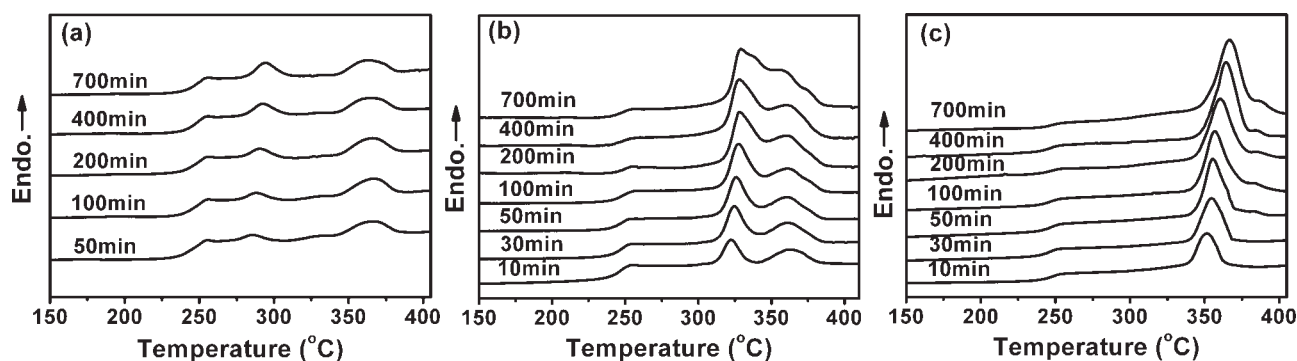
Figure 7 DSC subsequent heating curves of the PI annealed at (a) 260°C, (b) 300°C, and (c) 330°C for different times.

TABLE I
Melting Temperature of the PI Annealed at Different Temperature for Different Times

Crystallization time (min)	260°C		300°C		330°C	350°C
	T_{m1} (°C)	T_{m2} (°C)	T_{m1} (°C)	T_{m2} (°C)	T_m (°C)	T_m (°C)
10			322.3	360.4	351.4	367.4
30			324.8	360.4	354.5	370.4
50	285.2	365.9	325.9	360.0	355.5	371.4
100	288.2	365.9	327.3	360.4	356.9	373.9
200	290.2	365.9	327.9	360.9	360.4	376.9
400	292.7	365.4	328.4	360.9	364.5	380.4
700	294.2	365.4	329.4	360.5	366.5	383.4

However, for some weak transitions, DSC is not so sensitive to directly measure the exothermic heat. In this case, the samples are crystallized at predetermined temperatures for different periods of time, and then the heats of transition during subsequent heating process are measured. Using $(\Delta H)^{-1}$ versus $(\log t_c)^{-1}$ curve, one can obtain ΔH_∞ when t_c is infinite (here ΔH_∞ is used because crystallization time is infinite). The Avrami exponent n is computed using ΔH_∞ to substitute ΔH_0 by eqs. (1) and (2).

Figure 5(a–c) show the heating scans after the polyimide was crystallized at temperatures (T_c) ranging from 260 to 350°C after melt quenching from 376°C for 1 min. This range of T_c located between the T_g of PI sample and the melting temperature employed in this study. Figure 5(a) shows the DSC curves for the samples isothermally crystallized at 260°C. It can be seen that these curves only display prominent T_g at 246°C and without any endothermic peak during the subsequent heating process. This behavior is independent of crystallization time. The results not only indicate that the PI polymer chains cannot be rearranged to form a semicrystalline polymer at low crystallization temperature, but also showed that there is no recrystallization occurred during the cooling process.

When the samples were isothermally kept at 300°C for different times, the heat of transition during subsequent heating is calculated. From Figure 5(b), very interestingly, a new endothermic peak occurs when samples are subjected to isothermal crystallization for 100 min. Moreover, it can be seen that the DSC results are highly influenced by the crystallization time. The new endothermic peak shifts to higher temperature with the increase of crystallization time. The endothermic peak that appears at high temperature during the subsequent heating remains nearly at the same position. Here, we like to mention that a similar phenomenon has been found in other systems.[35–37] It is evident that all the crystals first developed have high melting points, i.e., the highest possible stability, whereas the crystals formed later melt much earlier, i.e., are less

stable. When the crystallization temperature is increased to 330°C, From Figure 5(c), it can be seen that the endothermic peak became more broad and obtuse. Both the heat of transition and the endothermic peak increase with the increase of crystallization time.

Because the crystallization process is too slow to be completed even in more than 700 min, the crystallization trace is hard to detect by DSC method. Figure 6 shows the corresponding Avrami plots for the various crystallization temperatures calculated from Figure 5(b) and 5(c) by eqs. (1) and (2). From Figure 6, we can see that the curves show an initial linear section but a change in the slop is observed at longer times. The straight-line fit through the initial section of the curves yields Avrami parameter n. The n value decreases slightly from 1.9 to 1.4 with increasing crystallization temperature from 300 to 330°C.

Effect of annealing

Figure 7 shows the DSC heating curves for the polyimide annealed at 260, 300, and 330°C for different times. From Figure 7(a), it can be seen that there
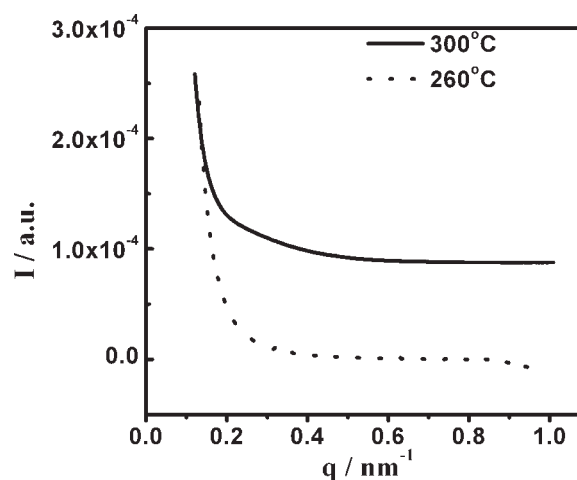
Figure 8 One-dimensionally integrated SAXS of the PI annealed at 260°C and 300°C for 50 min.
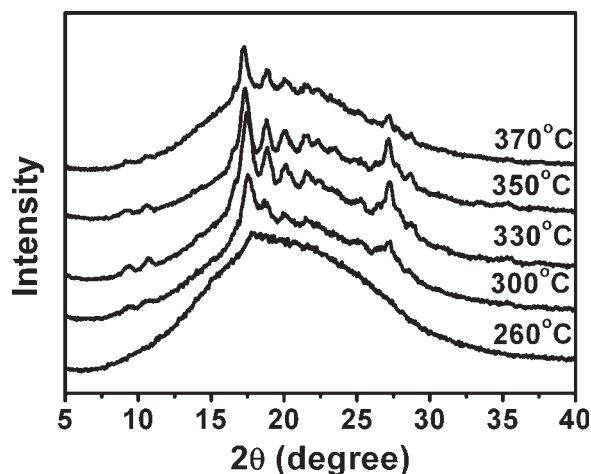
Figure 9 WAXD patterns of the PI annealed for 50 min at different temperatures.

appear two exothermic peaks. The heat transition of the first peak at low temperature increases slightly with increasing time, but the following peak at high temperature seems to be annealing-independent. The temperature difference between the two peaks is about 80°C. On increasing the annealing temperature to 300°C [from Figure 7(b)] we can also see that there are two exothermic peaks, and the heat transition increases with increasing annealing time. More-

over, the two exothermic peaks tend to close with the increase of annealing time, and eventually overlap with each other. The temperature difference between the two peaks under 300°C annealing is about 30°C, which is much smaller than that (80°C) under annealing at 260°C. The changes of exothermic peak are shown in Table I. This result indicates that the two endothermic peaks tend to close with increasing annealing temperature. When the annealing temperature is increased to 330°C or higher (350°C), only one peak appears as shown in Figure 7(c), indicating that the two exothermic peaks overlapped each other.

Most semicrystalline polymers exhibit multiple melting endotherms when crystallized/annealed at the temperature between T_g and T_m.[5,38,39] The lower melting endotherm is usually observed at 10–20°C above the crystallization temperature. Attempts to explain the origin of the multiple melting peaks in semicrystalline polymers have been made by various researchers. Two mechanisms have been proposed to explain the multiple melting behaviors. One is the reorganization model,[40–42] the other is the dual morphology model in which the secondary lamellae may melt at lower temperatures and the primary lamellae melt at higher temperatures.[43–46] Figure 8 shows the integrated one-dimensional SAXS pattern of the samples annealed at 260°C and 300°C for 50 min, respec-
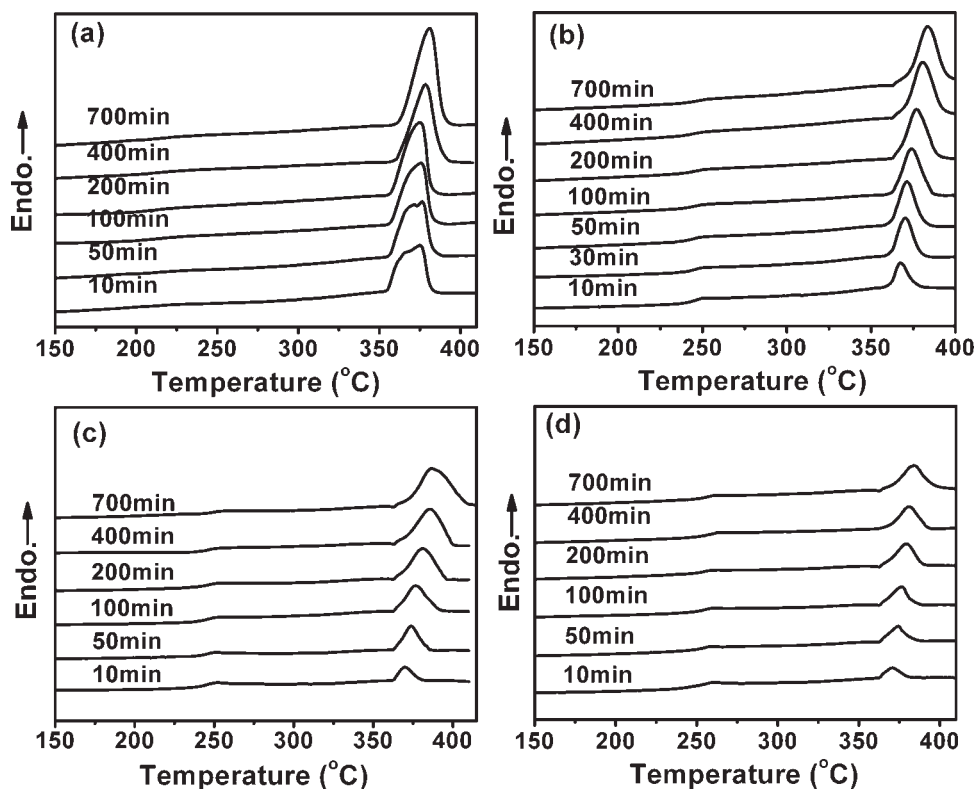
Figure 10 DSC subsequent heating curves of the PI isothermally annealed at 350°C for different times (η): (a) 0.34, (b) 0.46, (c) 0.51, (d) 0.55 dL/g.
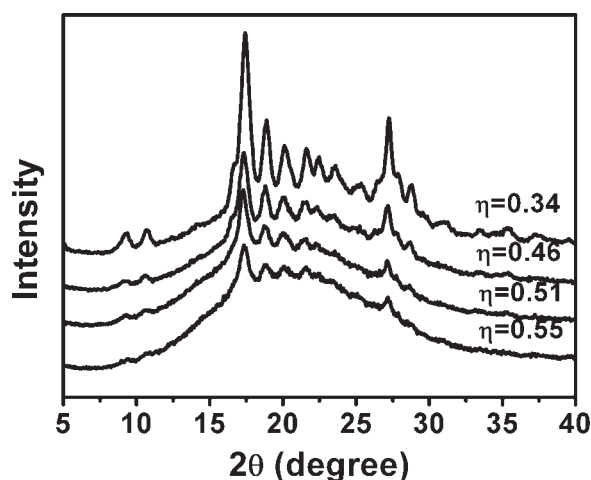
Figure 11 Evolution of WAXD patterns of the PI annealed for 50 min at 350°C with different inherent viscosities.

tively. It is indicated that there is no periodical crystalline lamella formed during the annealing process. So the double melting behavior of the PI may be attributed to the reorganization process. Since the low-temperature transition of the PI shifted continuously to a higher temperature as the annealing temperature increased, it cannot be attributed to a real melting of the as-formed crystals, but rather a partial disordering of weakly structured polymer chains. Similar results were reported in the Ref. 11. Therefore, the high-temperature transition can be ascribed to the final melting of the reorganized polymer crystals.

Figure 9 illustrates the structure evolution as a function of annealing temperature from 260 to 370°C by WAXD. When the samples are annealed at 260°C, a very faint reflection can be seen. When the samples are annealed at 300°C, we can observe the typical crystalline reflection. The reflection is stronger with increasing annealing temperature up to 350°C, thereafter it became weaker with further increase in annealing temperature. Moreover, from the results of WAXD patterns we can find that the diffraction peak positions remain unchanged with annealing temperature. This result indicates that the crystalline

form of the PI samples remains unchanged with annealing temperature.

Effect of inherent viscosity

To test the effect of the molecular weight on crystallization of the polyimide, a series of polyimide with different inherent viscosity were prepared by changing the amount of end-capper PA. Figures 10 and 11 show the subsequent DSC heating curves and WAXD patterns for the samples with inherent viscosity from 0.34 to 0.55 dL/g annealed at 350°C for different times. It is shown that the heat transition and the melting temperature are largely affected by inherent viscosity. The melting enthalpy decreases, whereas the melting temperature increases with increasing inherent viscosity, as shown in Table II. From Figure 11, we find that the reflection intensities decreased with increasing inherent viscosity, which is consistent with the result of Table I. Moreover, there is no significant difference for the peak positions, indicating that the PI samples with different inherent viscosities possess the same crystal unit cell.

CONCLUSIONS

Crystallization behavior of an aromatic thermoplastic polyimide derived from 3,3′,4,4′-ODPA and ODA have been studied by means of DSC. The results for nonisothermal crystallization study showed that the polyimide was difficult to recrystallize once taken to the melt. Isothermal crystallization results showed that a new exothermic peak appeared at lower temperature when the sample was subjected to isothermal crystallization for 100 min at 300°C. Moreover, the results indicated that the crystallization behavior was largely affected by crystallization temperature and time. Two melting endotherms appeared when annealing temperature was lower than 300°C. The two melting endotherms tended to close with increase in annealing temperature. When annealing temperature was higher than 330°C, only one melting endotherm appeared, indicating that the two exothermic peaks overlapped each other.

TABLE II
Thermal Properties of the PI with Different Inherent Viscosities Isothermally Annealed at 350°C for Different Times

Crystallization time (min)	$\eta = 0.34$ dL/g		$\eta = 0.46$ dL/g		$\eta = 0.51$ dL/g		$\eta = 0.55$ dL/g	
	T_m (°C)	ΔH_m (J/g)	T_m (°C)	ΔH_m (J/g)	T_m (°C)	ΔH_m (J/g)	T_m (°C)	ΔH_m (J/g)
10	374.8	29.71	367.4	8.66	370.0	4.60	370.5	4.50
50	374.9	34.32	371.4	18.05	374.0	9.90	374.5	6.65
100	375.7	36.12	373.9	20.73	376.4	13.47	376.4	8.34
200	376.5	39.00	376.9	24.15	379.4	18.50	381.4	11.90
400	378.4	45.58	380.4	26.43	380.8	22.77	383.4	14.16
700	380.8	55.29	383.4	28.49	384.0	26.63	385.5	16.26

References

1. Sroog, C. E. Prog Polym Sci 1991, 16, 561.
2. Hergenrother, P. M.; Stenzenberger, H. D.; Wilson, D. Polyimides; Blackie: London, 1990; p 58.
3. Mittal, K. L.; Ghosh, M. K. Polyimides, Fundamentals and Applications; Marcel Dekker: New York, 1996; p 7.
4. Ratta, V.; Stancik, E. J.; Ayambem, A.; Pavatareddy, H.; McGrath, J. E.; Wilkes, G. L. Polymer 1999, 40, 1889.
5. Srinivas, S.; Caputo, F. E.; Graham, M.; Gardner, S.; Davis, R. M.; McGrath, J. E.; Wilkes, G. L. Macromolecules 1997, 30, 1012.
6. Ratta, V.; Ayambem, A.; Young, R.; McGrath, J. E.; Wilkes, G. L. Polymer 2000, 41, 8121.
7. Cagiao, M. E.; Connor, M.; Baltá-Calleja, F. J.; Seferis, J. C. Polym J 1999, 31, 739.
8. Dorsey, K. D.; Desai, P.; Abhiraman, A. S.; Hinkley, J. A.; Clair, T. L. S. T. J Appl Polym Sci 1999, 73, 1215.
9. Srinivas, S.; Wilkes, G. L. Polymer 1998, 39, 5839.
10. Lu, S. X.; Cebe, P.; Capel, M. Polymer 1996, 37, 2999.
11. Song, N. H.; Yao, D. J.; Wang, Z. Y.; Sundararajan, P. R. Polymer 2005, 46, 3831.
12. Hsiao, B. S.; Sauer, B. B.; Biswas, A. J Polym Sci Part B: Polym Phys 1994, 32, 737.
13. Tsai, R. S.; Lee, D. K.; Liu, Y. C.; Tsai, H. B. J Appl Polym Sci 2003, 90, 2604.
14. Huo, P. P.; Friler, J. B.; Cebe, P. Polymer 1993, 34, 4387.
15. Friler, J. B.; Cebe, P. Polym Eng Sci 1993, 33, 587.
16. Ania, F.; Cagiao, M. E.; Baltá-Calleja, F. J. Polym J 1999, 31, 735.
17. Ratta, V.; Ayambem, A.; McGrath, J. E.; Wilkes, G. L. Polymer 2001, 42, 6173.
18. Heberer, D. P.; Cheng, S. Z. D.; Barley, J. S.; Lien, S. H. S.; Bryant, R. G.; Harris, F. W. Macromolecules 1991, 24, 1890.
19. Liu, X. K.; Tang, J. L.; Zheng, Y. Y.; Gu, Y. J Polym Sci Part B: Polym Phys 2005, 43, 1997.
20. Kreuz, J. A.; Hsiao, B. S.; Renner, C. A.; Goff, D. L. Macromolecules 1995, 28, 6926.
21. Hsiao, B. S.; Kreuz, J. A.; Cheng, S. Z. D. Macromolecules 1996, 29, 135.
22. Liu, S. L.; Chung, T. S.; Lu, L.; Torll, Y.; Oikawa, H.; Yamaguchi, A. J Polym Sci Part B: Polym Phys 1998, 36, 1679.
23. Ishida, H.; Huang, M. T. J Polym Sci Part B: Polym Phys 1994, 32, 2271.
24. Tamai, S.; Oikawa, H.; Ohta, M.; Yamaguchi, A. Polymer 1998, 39, 1945.
25. Sasuga, T. Polymer 1991, 32, 1539.
26. Torrz, L.; Maffezzoli, A.; Kenny, J. M. J Appl Polym Sci 1995, 56, 985.
27. Yudin, V. E.; Svetlichnyi, V. M.; Gubanova, G. N.; Didenko, A. L.; Sukhanova, T. E.; Kudryavtsev, V. V.; Ratner, S.; Marom, G. J Appl Polym Sci 2002, 83, 2873.
28. Brillhart, M. V.; Cebe, P. J Polym Sci Part B: Polym Phys 1995, 33, 927.
29. Li, Q. X.; Fang, X. Z.; Wang, Z.; Gao, L. X.; Ding, M. X. J Polym Sci Part A: Polym Chem 2003, 41, 3249.
30. Grenier, D.; Homme, R. E. P. J Polym Sci Polym Phys Ed 1980, 18, 1655.
31. Price, F. P. J Appl Phys 1965, 36, 3014.
32. Tomka, J. Eur Polym J 1968, 4, 237.
33. Hillier, I. H. J Polym Sci Part A: Polym Chem 1965, 3, 3067.
34. Banks, W.; Hay, J. N.; Sharples, A.; Thompson, G. Polymer 1964, 5, 163.
35. Strobl, G. Prog Polym Sci 2006, 31, 398.
36. Hauser, G.; Schmidtke, J.; Strobl, G. Macromolecules 1998, 31, 6250.
37. Ko, T. Y.; Woo, E. M. Polymer 1996, 37, 1167.
38. Chung, J. S.; Cebe, P. Polymer 1992, 33, 2312.
39. Chung, J. S.; Cebe, P. Polymer 1992, 33, 2325.
40. Blundell, D. J. Polymer 1987, 28, 2248.
41. Lee, Y.; Porter, R. S. Macromolecules 1987, 20, 1336.
42. Blundell, D. J.; Osborn, B. N. Polymer 1983, 24, 953.
43. Huo, P.; Cebe, P. Colloid Polym Sci 1992, 270, 840.
44. Cebe, P.; Chung, S. Polym Compos 1990, 11, 265.
45. Bassett, D. C.; Olley, R. H.; Al-Raheil, I. A. M. Polymer 1988, 29, 1745.
46. Cheng, S. Z. D.; Wu, Z. Q.; Wunderlich, B. Macromolecules 1987, 20, 2802.